

## Petrology, geochemistry and age dating of Skrut granitoids — new evidence for Early Triassic magmatism in Belasitsa Mountain (SW Bulgaria)

Nikola Zidarov<sup>1</sup>, Eugenia Tarassova<sup>1</sup>, Irena Peytcheva<sup>1</sup>,  
Albrecht von Quadt<sup>2</sup>, Valentin Andreichev<sup>3</sup>, Rositsa Titorenkova<sup>1</sup>

<sup>1</sup>Central Laboratory of Mineralogy and Crystallography, Bulgarian Academy of Science; 1113 Sofia;

E-mail: nzidarov@interbgc.com, etarassova@mail.bg, peytcheva@erdw.ethz.ch, rosititorenkova@dir.bg

<sup>2</sup>Institute of Isotope Geochemistry and Mineral Resources, ETH-Zurich, 8092 Zurich, quadt@erdw.ethz.ch

<sup>3</sup>Institute of Geology, Ural Division, Russian Academy of Sciences, 167982 Syktyvkar, Russia;

E-mail: izo@geo.komisc.ru

(Submitted: 17.04.2006; accepted for publication: 24.11.2006)

*Зидаров, Н., Тарасова, Е., Пейчева, И., Фон Квадт, А., Андрейчев, В., Титоренкова, Р. — Петрология, геохимия и возраст Скрытских гранитоидов — новые сведения о раннетриасовом магматизме в горном массиве Беласица (Ю-З Болгария). Скрытские гранитоиды обнажаются в западной части горного массива Беласица в Ю-З Болгарии. Интрузивные тела внедрены в биотитовые гнейсы и слюдяные сланцы, которые участвуют в сложной надвиговой структуре в рамках Сербо-Македонского массива. Главными породообразующими минералами гранодиоритов являются плагиоклаз, калиевый полевой шпат, кварц и биотит, а аксессуарными — апатит, алланит, эпидот, циркон, сфен и гранат. Породы испытали процессы динамометаморфизма и неравномерное гидротермальное изменение. По содержанию  $K_2O$  относятся к высококалиевой известково-щелочной магматической серии, а по ASI коэффициенту — к слабопералюминиевым гранитоидам. Магма была водонасыщенной и богатой на REE. Кристаллизация, вероятно, протекала при давлении 11–11.5 kbar (присутствие магматического эпидота) и в температурном интервале 800–600°C. Положительные значения  $\epsilon\text{-Hf}$  циркона (от +0.4 до +3.5) предполагают вулканическую дуговую/океанскую континентальную или постколлизийную обстановку образования магмы.*

Возраст гранитоидов  $248.85 \pm 0.70$  Ма определен конвенциональным U–Pb методом по циркону. Линия регрессии по данным Rb–Sr изотопного анализа валовых проб отвечает наклону в  $167.3 \pm 8.1$  Ма и интерпретируется как линия смешения, вероятно испытывавшая влияние наложенных процессов. Новые данные предполагают формирование Скрытских гранитоидов в раннем триасе в результате позднегерцинского проявления экстензии и блокового расчленения (рифтинга). Постметаморфическое внедрение гранитоидов определяет дотриасовый возраст метаморфизма высокой степени в районе горного массива Беласица.

*Abstract.* The Skrut granitoids crop out in the western part of Belasitsa Mountain in SW Bulgaria. They are intruded in biotite gneisses and mica schists, building up together a complex nappe structure in the frame of the Serbo-Macedonian Massif (SMM). Main rock forming minerals in the Skrut granitoids are plagioclase, potassium feldspar, quartz, and biotite and accessories are apatite, allanite, epidote, zircon, titanite and garnet. These granitoids have undergone processes of dynamic metamorphism and non-uniform hydrothermal alteration. In respect to  $K_2O$  content they belong to the high potassium calc-alkaline magmatic series while according to the ASI coefficient they are related to the weakly per-aluminium granitoids. The magma is enriched in water and REE. Probably, its crystallization has proceeded at pressure of 11 to 11.5 kbar (presence of magmatic epidote) and temperature of 800 to 600°C. The positive  $\epsilon\text{-Hf}$  values of zircon crystals (from +0.4 to +3.5) propose mixed crust-mantle magma source whereas calc-alkaline characteristics and discrimination diagrams propose a volcanic-arc/continental margin or post-collisional environment of the magma generation.

The age of the granitoids is determined by conventional U–Pb method on zircons as  $248.85 \pm 0.70$  Ma. The regression line obtained by the Rb–Sr isotope analyses on whole rock samples yield an age of  $167.3 \pm 8.1$  Ma, which is interpreted as a mixing line, probably influenced also by overprinted events. The new data suggest formation of the Skrut granitoids during the Early Triassic as a result of Late Variscan event in extensional conditions and block dismembering (rifting?). The post-metamorphic intrusion of the granitoids defines the high grade metamorphism in Belasitsa Mountain as pre-Triassic in age.

Zidarov, N., Tarassova, E., Peytcheva, I., von Quadt, A., Andreichev, V., Titorenkova, R. 2007. Petrology, geochemistry and age dating of Skrut granitoids — new evidence for Early Triassic magmatism in Belasitsa Mountain (SW Bulgaria). — *Geologica Balc.*, 36, 1–2; 17–29.

**Keywords:** granodiorites, Serbo-Macedonian Massif, U-Pb and Rb-Sr dating, isotope geochemistry, conditions of formation, geodynamic environment.

## Introduction

Several small bodies of porphyric granodiorites designated as Skrut pluton crop out on an area of about 13 km<sup>2</sup> in the western part of Belasitsa Mountain, south of Skrut and Gabrene villages (Fig. 1).

A first publication of these intrusive bodies was done by Bonchev (1920). Later this area has been mapped in a scale 1:25 000 by Zidarov et al. (1965), providing the first petrographic data about Skrut granitoids. Further informations about the granitoids are given on the geological map of Bulgaria (in a scale 1:100 000) and the accompanying explanatory note (Zagorchev, Dinkova, 1990, 1991).

The present investigation includes a summary of mineralogical and petrographic characteristics of the Skrut granitoids. A combination of isotope methods — U-Pb zircons and Rb-Sr whole rock analyses — is used to detect the age of the granitoid protholith. The magma sources are characterized by the initial Sr ratios as well as the  $\epsilon$ -Hf values of the dated zircons.

## Geological setting and sampling

Skrut granodiorites are an integral part of Belasitsa horst, which crops out in the southern part of Ograzhden block of Serbo-Macedonian Massif (SMM)

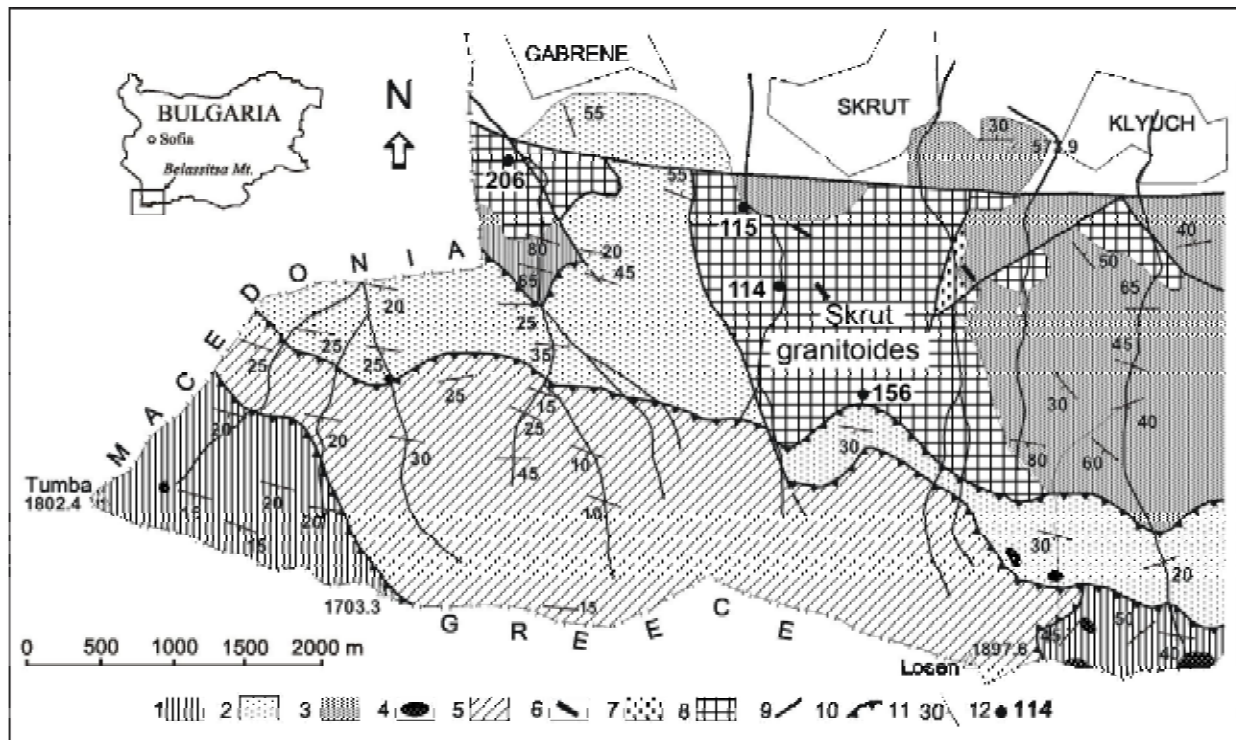


**Fig. 1.** Geological map of the Western part of Belasitsa Mt. (after Zidarov et al., 1966 and Zidarov, Angelski, 1995, unpublished report). 1 — amphibolites; 2 — two-mica gneisses and schists; 3 — biotite gneisses; 4 — serpentinite bodies; 5 — metagranites; 6 — granodiorite-porphry dykes; 7 — fine-grained granodiorites; 8 — Skrut porphyritic granodiorite; 9 — fault; 10 — thrust; 11 — schistosity; 12 — sample locations and No of sample

(Zagorchev, 2001). The horst is situated between Podgorie and Butkovo faults separating it respectively from the Strumeshnitsa graben to the north and Serres graben to the south, which are filled with Neogene and Quaternary sediments (Zagorchev, 1992). The horst is built up of rocks of the Ograzhdenian complex, which are metamorphosed in amphibolite facies (Kozuharov et al., 1974; Zagorchev, 1976) and later intruded by the Skrut granitoids. The metamorphic rocks are represented by medium- to small-grained biotite gneisses and by the overtrusted two-mica gneiss-schists and schists (Fig. 1). Upon them in a superposition there are two nappe plates, dipping to south and built up of metagranites and amphibolites (Fig. 1).

The contact between Skrut granitoids and their host metamorphic rocks is usually covered by eluvium. The observed field relationships indicate the existence of a tectonic contact, as they are observed along the western boundary of the big outcrop south of Skrut village (Fig. 1). Granitoids are cross-cut by granodiorite porphyry dykes and small quartz veins. Another small body of fine-grained granodiorites, similar to the granitoids, cropping out near the Yavornitsa village (Tarassova et al., 2001), is emplaced along the eastern contact.

The Skrut granitoids are marked by negative gravity and magnetic anomalies (Dimovski, Sevdanov, 2002).

For the present study the Skrut granitoids were sampled in the big outcrop south of Skrut village as well as in the small bodies south of Gabrene and Klyuch villages (Fig. 1).

## Petrology and mineralogy

The studied rocks were determined as granodiorite according to the modal classification of Le Maitre et al. (1989) (Fig. 2). They are leuco- to mesocratic with massive to fluidal texture and granitic structure and are medium-grained, porphyric after K-feldspar, irregularly deformed and hydrothermally altered. The porphyries reach up to 10 cm in length. They are orientated parallel to the schistosity in more intensively deformed parts.

Main rock-forming minerals are plagioclase (30–50%), K-feldspar (6–22%), quartz (16–30%), and biotite (9–22%). Accessory minerals (0.6–1.2%) are apatite, allanite, zircon, members of the epidote-clinozoisite series, titanite and garnet. The secondary minerals are represented by fine-flaky biotite, epidote, chlorite, sericite, pyrite and quartz.

*Plagioclase* is of oligoclase composition ( $An_{20-25}$ ) and is represented by euhedral crystals with lamellar structure (Table 1, analysis 1). Sometimes they are cracked and slightly bended with undulatory extinction and masked lamellae. *Potassium feldspar* is represented by fine-grained and porphyry microcline with cross-hatched structure (Table 1, analysis 2) and includes plagioclase, biotite, quartz, zircon and veinlets of fine-grained microcline, chlorite, and epidote.

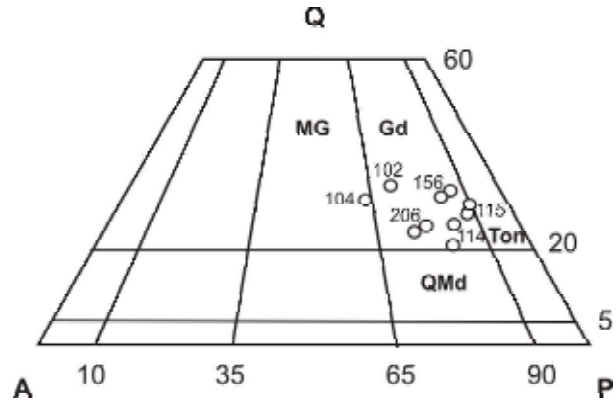


Fig. 2. Modal composition of Skrut granodiorites (Le Maitre et al., 1989): Gd – granodiorite; MG – monzogranite; QMd – quartz-monzodiorite; Ton – tonalite

At the boundary between microcline and plagioclase there are formed myrmekites. *Biotite* displays  $fm=100 \cdot Fe_{tot}/(Fe_{tot} + Mg)$  of 50–58 and low content of titanium –  $TiO_2$  up to 2.43 wt.% (Table 1, analyses 3 and 4; Fig. 3). It is replaced by muscovite and rarely, by fine-grained epidote and in some parts by chlorite. *Quartz* is transparent and with undulatory extinction.

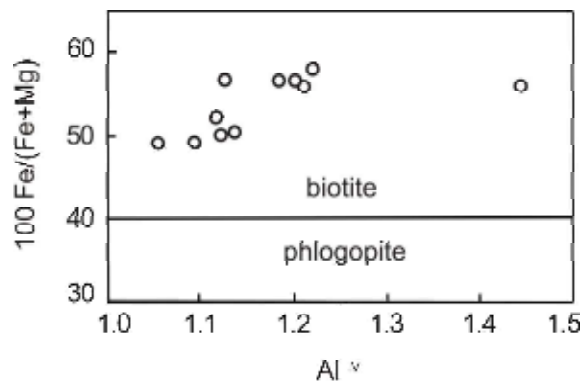


Fig. 3. Compositions of biotites from Skrut granodiorites on the plot  $100 \cdot Fe/(Fe + Mg)$  versus  $Al^{IV}$

The relations between the main rock-forming minerals determine a row of consecutive crystallization as follows: plagioclase → biotite → quartz → K-feldspar.

*Apatite* is the most widespread accessory mineral. It is small prismatic, associates with biotite and is included in microcline and allanite. *Zircon crystals* with predominantly developed prism {110} and bipyramid {101} (Fig. 4a, b) are found in quartz, microcline and biotite, and some of them contain biotite flakes. *Zircon* grains display the presence of an oscillatory zoning, typical of magmatic growth conditions, without any signs of dissolution of the surface (Fig. 4c and Fig. 9). The latter is an indication for high saturation of Zr in the melt. The predominating morphotypes according to the method of Pupin (1980) are  $S_4$ ,  $S_5$ ,  $S_8$ ,  $P_1$ ,  $P_3$ , and  $G_1$  (Fig. 5). The typologic evolution starts with sub-types  $S_{14-15}$ , passes

Table 1  
Selected microprobe analyses of minerals from Skrut granodiorites

mineral	Pl		Kfsp		Bi		Allan I		Ep		Grt	
	1	2	3	4	5* (core)	6* (rim)	7*	8	9			
SiO <sub>2</sub>	62.11	65.85	39.98	39.29	32.4	32.7	38.0	37.16	37.23			
TiO <sub>2</sub>			2.21	1.82	1.3	0.80	0.09					
Al <sub>2</sub> O <sub>3</sub>	24.79	18.47	18.38	17.71	16.9	18.4	26.7	21.02	21.42			
FeO <sub>tot</sub>			18.59	21.88	12.5	11.4	6.7	20.93	18.91			
MnO								4.52	6.79			
MgO			10.37	9.09	1.1	0.75	0.28	1.00	0.96			
CaO	4.59				11.3	12.2	22.0	14.05	14.43			
Na <sub>2</sub> O	8.80	15.81										
K <sub>2</sub> O	0.17		9.35	9.43								
Y <sub>2</sub> O <sub>3</sub>					0.49	0.48	0.60					
La <sub>2</sub> O <sub>3</sub>					5.0	4.7	0.31					
Ce <sub>2</sub> O <sub>3</sub>					11.2	9.9	1.0					
Pr <sub>2</sub> O <sub>3</sub>					1.2	1.0						
Nd <sub>2</sub> O <sub>3</sub>					4.3	2.9	0.69					
Sm <sub>2</sub> O <sub>3</sub>					0.72	0.45						
Gd <sub>2</sub> O <sub>3</sub>					0.70	0.32						
ThO <sub>2</sub>					0.79		0.11					
UO <sub>2</sub>						1.1	0.33					
total	100.46	100.13	98.88	99.22	99.9	100.2	96.8	98.68	99.74			
Formula calculation per O												
	8		11		12,5		12					
Si	2.736	3.02	2.879	2.872	2.976	2.992	3.016	2.979	2.951			
Ti			0.120	1.128	0.088	0.055	0.005					
Al <sup>IV</sup>	1.086	0.998	1.121	0.396				0.021	0.049			
Al <sup>VI</sup>			0.438	0.1	1.823	1.980	2.498	1.964	1.951			
Fe			1.120	1.337	0.963	0.870	0.447	1.403	1.254			
Mn								0.307	0.456			
Mg			1.113	0.990	0.150	0.102	0.033	0.12	0.113			
Ca	0.217				1.115	1.195	1.875	1.207	1.226			
Na	0.752											
K	0.010	0.925	0.859	0.879								
Y					0.024	0.023	0.025					
La					0.170	0.158	0.009					
Ce					0.376	0.330	0.029					
Pr					0.041	0.034						
Nd					0.140	0.095	0.020					
Sm					0.023	0.014						
Gd					0.021	0.010						
Th					0.016	0.064	0.002					
U						0.021	0.006					
fm			50	57								
Ab	76.90	0.00										
An	22.10	0.00										
Or	1.00	100.00										
Ep							48					
Alm								46	41			
Grs								40	40			
Sps								10	15			
Prp								4	4			

Pl — plagioclase, Kfsp — potassium feldspar, Bi — biotite, Allan — allanite, Ep — epidote, Grt — garnet

\*Analyses 5, 6, 7 after Тарасова, Тарасов (2004);

The chemical composition of minerals was analyzed with a Philips SEM-515 equipped with an EDAX 9100/70 analytical system (CLMK — BAS) using the FRAME-C ZAF-correction program. Operating conditions were 18 kV acceleration voltage, 35° sample tilt, 51,3° take-off angle.

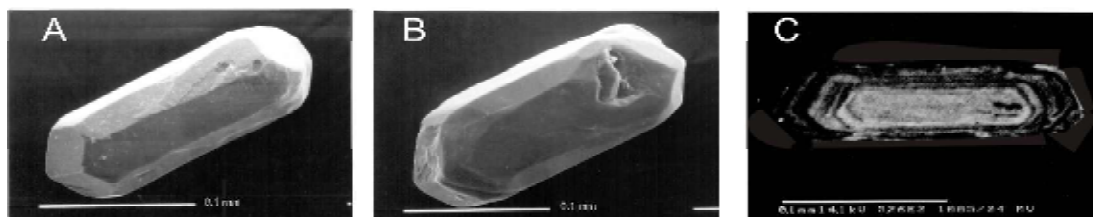


Fig. 4. Morphology and internal texture of zircon crystals: a) S<sub>14</sub> subtype, sample 115 (x 500); b) S<sub>3</sub> subtype, sample 114 (x500); c) oscillatory magmatic zonation — SEM-CL image, cross-section parallel to (110) plane

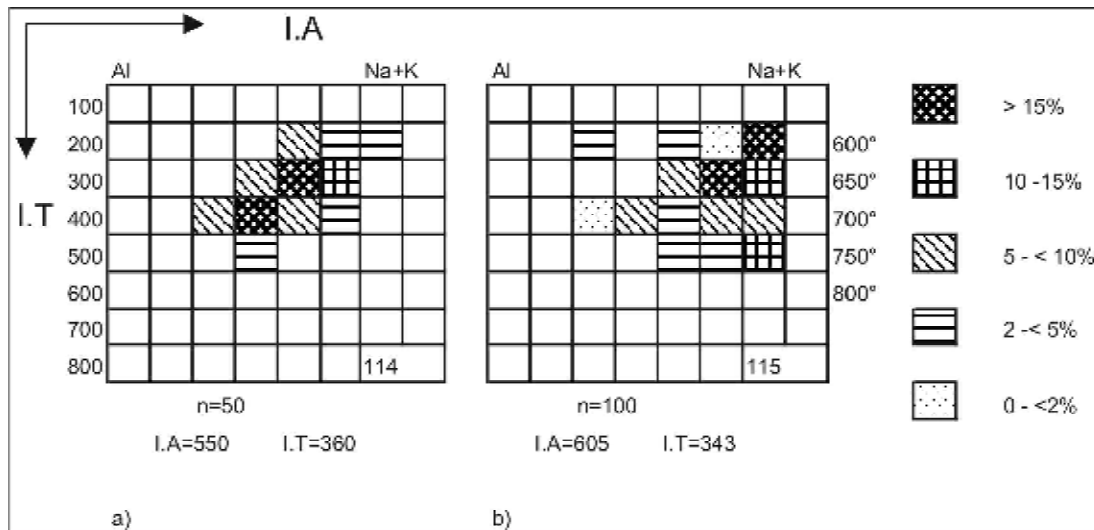


Fig. 5. Typologic distribution of the studied zircon populations (samples 114, 115)

through  $S_{4-5}$  and ends with  $G_1$ . Zircon populations are characterized by relatively low temperature indices I.T (340–360) and higher values of the index I.A (550–600). Garnet is of almandine-grossular composition  $Alm_{41-46}Gross_{38-40}Spess_{10-15}Pyr_4$  (Table 1, analyses 8 and 9), forms metacrystals, which contain inclusions of biotite and quartz but later replaced by epidote and chlorite. Titanite forms either big euhedral crystals or fine-grained aggregates. Ce-allanite is observed in two varieties (Tarassova, Tarassov, 2004). The earlier one is represented by prismatic crystals, which are richer in REE and poorer in Th, compared with the later variety, which is encountered as anhedral grains (Table 1, analyses 5 and 6). This allanite usually associates with biotite, includes apatite and apparently crystallizes before plagioclase. The epidote-clinozoisite series of minerals — Ep 35–65 mol % (Table 1, analysis 7) overgrow and replace both allanite varieties. They also crystallize independently with their crystals being euhedral along the boundary with biotite but corroded along the boundary with plagioclase. This is an indication for their early magmatic origin (Schmidt, Thompson, 1996).

## Petrochemistry

According to the TAS classification diagram (Bogatikov et al., 1981) all rocks have chemical composition corresponding to granodiorites (Table 2, samples 114, 156, 680). Some deviations towards the composition of alkaline granites (sample 206) and quartz-diorites (sample 115) are probably caused by local heterogeneities based on uneven assimilation of continental crust material or through magma mixing. In respect to  $K_2O$  content (3.12–4.26%) they relate to the high-potassium calc-alkaline magmatic series (Peccerillo, Taylor, 1976). The values of the ASI coefficient (mean 1.07) and the composition on the

Table 2

Major elements compositions (wt. %) and CIPW norms of selected Skrut granodiorites

Sample	156	114	680	115	206
major elements, wt %					
SiO <sub>2</sub>	66.80	66.50	64.68	61.60	68.40
TiO <sub>2</sub>	1.00	0.22	0.5	0.75	0.65
Al <sub>2</sub> O <sub>3</sub>	15.12	16.85	15.15	16.92	15.30
Fe <sub>2</sub> O <sub>3</sub>	1.64	1.57	4.26	3.03	1.26
FeO	2.16	1.78	1.97	1.68	1.70
MnO	0.06	0.04	0.22	0.09	0.04
MgO	1.33	0.92	1.55	2.03	0.98
CaO	2.66	2.39	2.28	4.48	0.70
Na <sub>2</sub> O	3.78	4.46	3.11	3.57	4.20
K <sub>2</sub> O	3.12	3.27	4.61	3.03	4.70
P <sub>2</sub> O <sub>5</sub>	0.20	0.10	0.16	1.53	0.10
LOI	0.89	1.30	1.09	1.82	1.66
total	98.76	99.40	99.58	100.53	99.69
CIPW					
q	25.3	21.1	22.2	20.9	22.9
or	18.4	19.3	27.2	17.9	27.7
ab	32.0	37.7	26.3	30.2	35.5
an	11.9	11.2	10.3	12.3	3.5
C	1.2	1.9	1.3	3.2	2.3
D.I.	75.7	78.1	75.7		86.1
ASI*	1.05	1.11	1.06	0.98	1.15
trace elements, ppm					
Rb	146	140	-	117	179
Sr	161	193	-	384	176
Nb	14	<10	-	11	11
Zr	176	257	-	159	171
Y	14	14	-	11	<10
compositions of rocks					
chemical	Gd	Gd	Gd	Qd	G
modal	Gd	Gd	Gd	Gd	Gd

The main rock forming oxides were determined by wet chemical analysis and atomic absorption spectrometry (AAS) in CLMC. The content of minor elements, Rb, Sr, Zr, Y and Nb was determined by X-ray fluorescence analysis in Research Center Eurotest PLC, Bulgaria; ASI =  $Al_2O_3 / (CaO + K_2O + Na_2O)$  (mol. %) is calculated without correction for the CaO content in apatite; The abbreviations are as follows: G — granite, Gd — granodiorite, Qd — quartz-diorite; Analyse 680 after Zidarov et al. (1966).

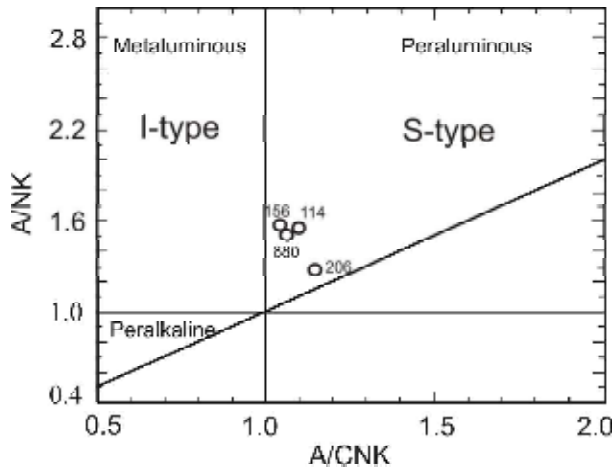


Fig. 6. Element compositions of the Skrut granodiorites plotted on the A/NK — A/CNK diagram of Maniar & Piccoli (1989)

diagram of Maniar, Piccoli (1989) determine them as slightly per-aluminous S-type (Fig. 6). This explains the existence of normative corundum (Table 2). The biotite composition (Table 1, Fig. 7) is transitional between the calc-alkaline and per-aluminous granite fields according to the diagram of Abdel-Rahman (1994). The typological trend of the zircons (Pupin, 1980, Fig. 5) also supports the conclusion that these rocks belong to the calc-alkaline series. The relatively high I.A and the low I.T indexes of the zircon population as well as the predominant development of the {101} bipyramid correspond to the high alkalinity of the magma.

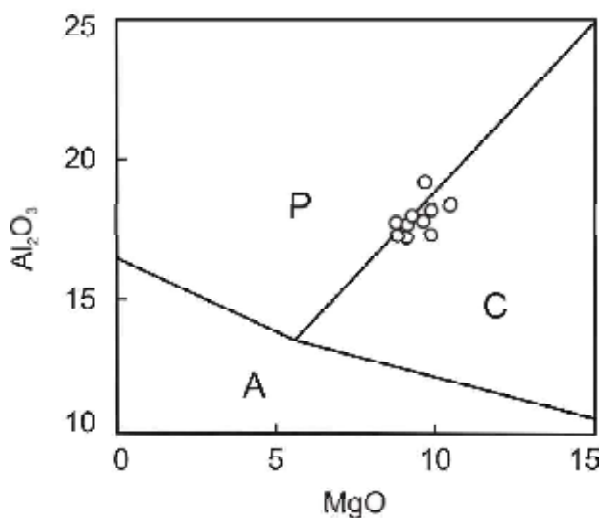


Fig. 7. Position of biotites from Skrut granitoids on the discriminant diagram  $Al_2O_3$  vs.  $FeO_{tot}$  (wt. %) of Abdel-Rahman (1994). Fields of discriminated granites: A — alkaline; C — calc-alkaline; P — peraluminous

## Post-magmatic processes and products

**Dynamometamorphism.** Skrut granitoids are irregularly brittle and brittle-ductile deformed, which led to formation of foliation. On a micro-scale this is expressed in fracturing, bending, masking of the lamella and undulatory extinction of plagioclases; fracturing and undulatory extinction of the quartz grains; bending of biotite around microcline. In the mostly deformed parts the biotite is changed to muscovite, epidote and chlorite, the plagioclase — to sericite and chlorite, and the garnet — to epidote and chlorite. Myrmekites are observed along the boundary of plagioclase and K-feldspar. These mineral assemblages characterize a greenschist to lower amphibolite facies metamorphism.

**Hydrothermal alterations** are observed along a tectonic zone, which fledge the Podgorie fault to southwest of Klyuch village (length of 1800 m and width of 30 to 120 m). The mineral parageneses define greisenization and sericitization processes (Pirajno, 1992). K-silicate alteration led to formation of potassium feldspar and biotite after plagioclase. With increase of the acidity of the hydrothermal solution the feldspar minerals and biotite had become more unstable and changed to muscovite and quartz (quartz-muscovite facies of greisens, Zharikov, Ome-lyanenko, 1978). The greisens are composed of muscovite (radial aggregates), coarse-grained xenomorphic quartz and random fluorite, tourmaline, beryl, cassiterite, molybdenite, and scheelite. These greisens are not of economical significance.

The sericitization, characterized by the mineral paragenesis of quartz, sericite, and pyrite (Pirajno, 1992) is unevenly developed, sometimes overprinting the greisenized rocks. Pyrite and quartz, and rarely chalcopyrite form nests and veinlets.

## Isotope geochronology and geochemistry

### U-Pb zircon dating

Conventional U-Pb dating was performed in the Institute of Isotope Geology and Mineral Resources of ETH-Zurich using ID-TIMS (Isotope Dilution — Thermal Ionization Mass Spectrometry) technique on zircon crystals from sample 115 (Fig. 1). Prismatic beige zircon crystals were selected for analysis, which are characterized by predominance of the bipyramid {101} and prism {110} faces. Two of the measured zircon grains were in addition mechanically abraded in order to remove eventual outer zones with radiogenic lead losses. The results are shown in Table 3 and Figure 8. The program ISOPLOT was used for processing the data and calculation of the age (Ludwig, 1998). All points, which correspond to both abraded and non-abraded zircons are concordant or negligibly discordant and determine an Early Triassic age of  $248.85 \pm 0.70$  Ma (Fig. 8, Table 3, Peytcheva et al., 2005). This age is in a good agree-

Table 3  
U-Pb zircon isotope data for sample B-115 of Skrut granodiorite, Belasitsa mountain

N	Size fraction, $\mu\text{m}$	weight in mg	#	U ppm	Pb ppm	$^{206}\text{Pb}/^{204}\text{Pb}$	$^{206}\text{Pb}/^{238}\text{U}$	$2\sigma$ error %
<b>B-115</b>								
1	-125+70	0.0035	prism transp brownish	318	15.5	210.1	0.039372	0.48
2	-125+70	0.0035	prism transp brownish	219	8.81	952.0	0.039232	0.47
3	-125+70	0.0037	long prism brownish abr	206	8.56	772.4	0.039455	0.79
4	-125+70	0.0039	long prism brownish abr	138.4	8.20	136.7	0.039535	0.59
	$^{207}\text{Pb}/^{235}\text{U}$	$2\sigma$ error %	$^{207}\text{Pb}/^{206}\text{Pb}$	$2\sigma$ error %	$^{206}\text{Pb}/^{238}\text{U}$	$^{207}\text{Pb}/^{235}\text{U}$	$^{207}\text{Pb}/^{206}\text{Pb}$	Rho
					apparent ages			
1	0.275727	1.33	0.050792	1.19	248.9	247.3	231.4	0.44
2	0.276055	0.60	0.051034	0.37	248.1	247.5	242.4	0.79
3	0.278081	0.99	0.051117	0.60	249.5	249.1	246.1	0.80
4	0.276640	4.79	0.050750	4.58	249.9	248.0	229.5	0.41

#: abr – abraded, prism – prismatic, abr – abraded grains; transp – transparent; Rho – correlation coefficient  $^{206}\text{Pb}/^{238}\text{U} - ^{207}\text{Pb}/^{235}\text{U}$

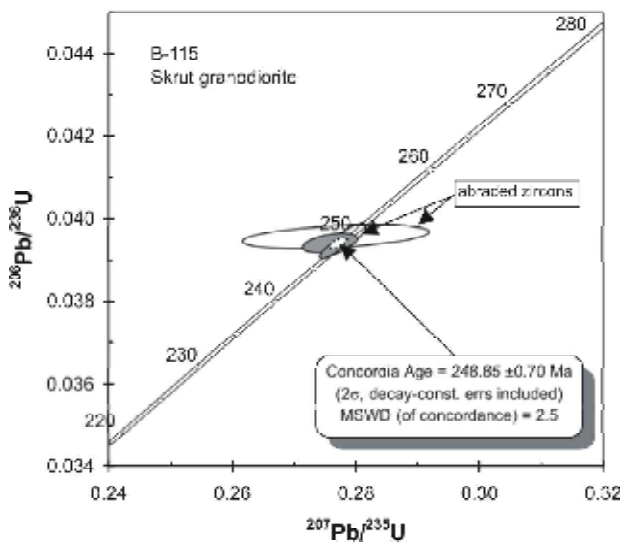


Fig. 8. Concordia diagram for zircons from sample B-115 of Skrut granitoids

Table 4  
Hf isotope data for zircons from sample B-115 of the Skrut granodiorite (numbers as in Table 3)

Sample N	$^{176}\text{Hf}/^{177}\text{Hf}$	$2\sigma$ error	$\epsilon\text{-Hf}$ today	$\epsilon\text{-Hf}$ T 250
B115/4	0,282674	0,000012	-3,47	1,20
B115/1	0,282738	0,000012	-1,20	3,46
B115/2	0,282652	0,000044	-4,24	0,42

\*For the calculation of the  $\epsilon\text{-Hf}$  values the present-day ratios  $(^{176}\text{Hf}/^{177}\text{Hf})_{\text{CH}} = 0.28286$  and  $(^{176}\text{Lu}/^{177}\text{Hf})_{\text{CH}} = 0.0334$  are used, and for 250 Ma and  $^{176}\text{Lu}/^{177}\text{Hf}$  ratio of 0.0050 for all zircons was taken into account.

ment with the *in-situ* LA-ICP-MS analyses of zircons from samples 114 and 115. The calculated values for  $^{206}\text{Pb}/^{238}\text{U}$  in different parts of the selected prismatic crystals define ages between 220 and 300 Ma (the ratios  $^{207}\text{Pb}/^{235}\text{U}$  in the same zircons measured with greater uncertainty leading to discordant position of the corresponding points, to the right of the concordia line).

#### Hf-isotope tracing and distribution of REE in zircons

The isotopic hafnium ratios were measured for some of the analyzed zircon crystals in order to characterize the magma source from which the zircons have crystallized. The positive values of  $\epsilon\text{-Hf}$  range from +0.4 to +3.5 (Table 4) argue for mixed crust-mantle source of magma.

The chondrite-normalized distributions of the rare earth elements (REE) in zircons from rock samples 114 and 115 are similar to one another and are typical of unaltered igneous zircon (Hoskin, Ireland, 2000, Belousova et al., 2002) characterized by depletion in light elements (LREE) and steep enrichment in heavy elements (HREE) (Fig. 9). The positive Ce anomaly gives evidence for positive oxidation potential of magma while the negative Eu anomaly should be related to fractionation of plagioclase.

The areas with a higher intensity of cathodoluminescence (bright areas in CL images) in zircon crystals B114-2 and B115-3 exhibit a lower content of trace elements and especially of uranium. These areas are developed around inherited cores which according to the preliminary *in-situ* LA ICP-MS analyses are of Early Paleozoic age, and their chondrite-normalized plots are characterized with a certain

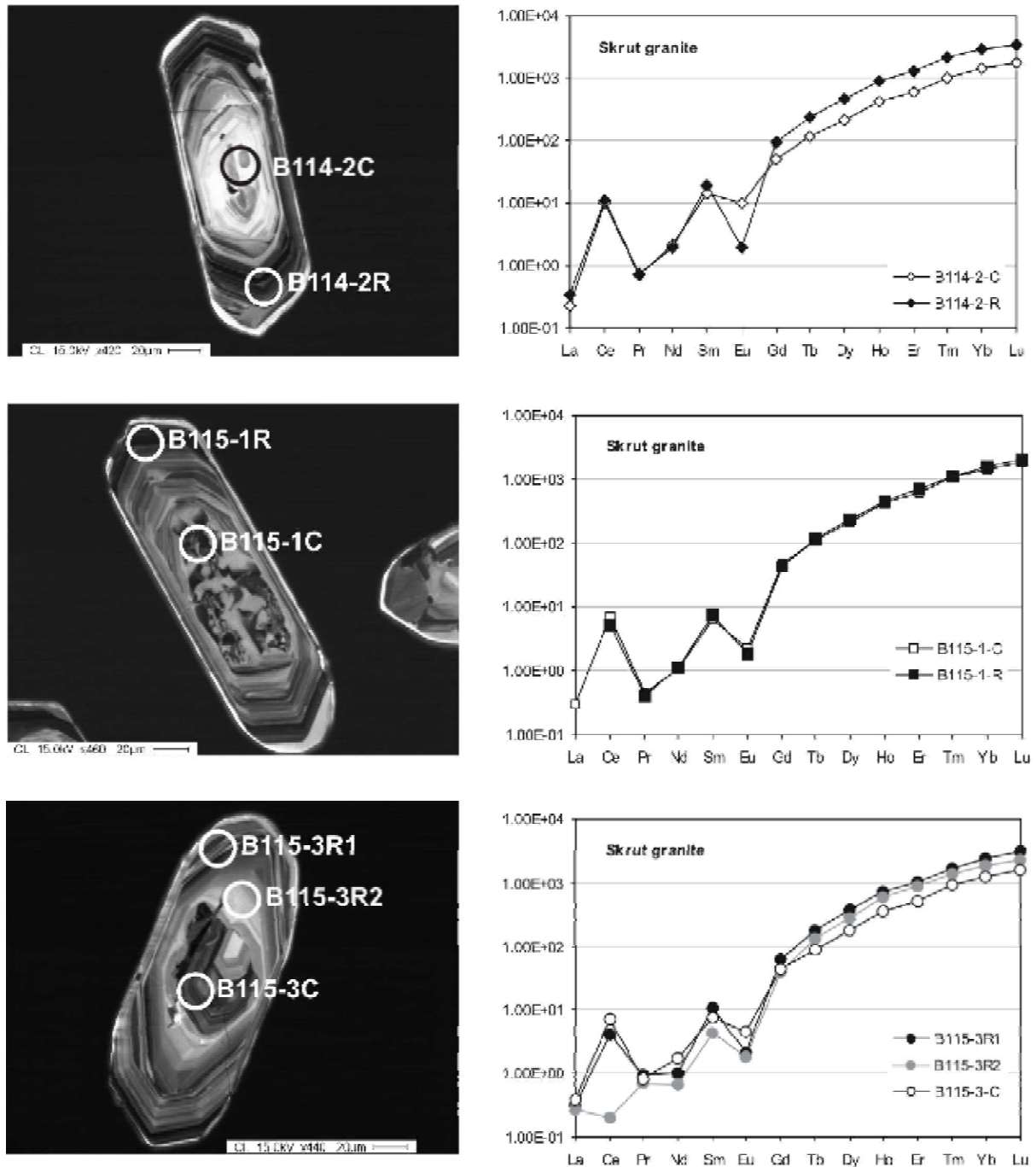


**Fig. 9.** Cathodoluminescence (CL) images of zircons from samples B-114 and B-115 of Skrut granodiorite with the corresponding chondrite-normalized REE distribution. Circles on the pictures correspond to the laser-ablation spot in the zircon crystals.

depletion of REE. In some cases, the positive Ce anomaly disappears due to the LREE relative depletion (Fig. 9 – B115-3R2). Such a kind of REE pattern is characteristic of altered igneous zircon. In other cases, the normalized REE patterns are relatively HREE-depleted and the negative Eu anomaly becomes weakly expressed as seen for the inherited core in zircon (Fig. 9 – B114-2C). The presence of inherited cores and altered areas in zircon crystals

are an additional evidence for participation of crust material in the granitoid magma generation and of secondary alteration processes.

#### Rb-Sr isotope dating and geochemistry

Whole rock Rb-Sr analyses of four representative samples (Table 5) were performed in the Geochro-

Table 5  
Rb-Sr data for whole rock samples of Skrut granitoids.

Sample N	Rb (ppm)	Sr (ppm)	$^{87}\text{Rb}/^{86}\text{Sr}$	$^{87}\text{Sr}/^{86}\text{Sr} \pm 2\sigma$
156	156.9	164.5	2.762	0.71973 $\pm$ 0.00014
114	136.9	197.1	2.011	0.71812 $\pm$ 0.00020
115	116.3	390.9	0.861	0.71523 $\pm$ 0.00016
206	166.3	189.0	2.547	0.71927 $\pm$ 0.00024

nological Laboratory of RAS in Syktyvkar. The contents of Rb and Sr were determined by the method of isotope dilution using a  $^{87}\text{Rb}/^{84}\text{Sr}$  tracer. After dissolving of the samples in a mixture of HF and HCl the separation of concentrates of Rb and Sr on chromatographic columns was performed with ion-exchange resin DOWEX 50x8 (200–400 mesh). The blanks of  $^{87}\text{Rb}$  and  $^{86}\text{Sr}$  do not exceed 0.5 ng. The measurements are performed on MI-1201 mass-spec-

trometer applying single-ray method in a double rhenium filament regime of ionization. The measured isotope ratios of Sr are normalized according to  $^{86}\text{Sr}/^{88}\text{Sr} = 0.1194$ . Fractionation correction was not applied during the measurement. The NBS 987 measurements during this project give an  $^{87}\text{Sr}/^{86}\text{Sr}$  value of  $0.71026 \pm 0.00002$  (1s). The discrepancy in the  $^{86}\text{Rb}/^{88}\text{Sr}$  determination is 1.5% (1s). ISOPLOT program (Ludwig, 1998) was used for the calculation of the isotopic parameters.

The obtained results are given in Table 5. The data points of the samples 114, 115, 156, and 206 determine a regression line (Fig. 10a), which slope corresponds to an age of  $167.2 \pm 8.1$  Ma. The age differs significantly from that of the U-Pb zircon analyses. As far as the latter is one of the most precise methods for dating of magmatic rocks then a question remains if the obtained Jurassic age has a geological significance (reflects a proper geological event in the history of the studied irregularly deformed granodiorites) or describes a “false” age being a result of primary mixing of magmas with different isotopic characteristics or is due to strontium losses during secondary processes.

A conventional test was performed in order to check the validity of the obtained Rb-Sr isochrone for the Skrut granitoids by constructing a diagram in coordinates —  $(1/\text{Sr} \cdot 1000)$  versus  $(^{87}\text{Sr}/^{86}\text{Sr})$ . Although with higher MSWD=14 (Fig. 10b) the points again determined a line, which points to a probable mixing of magmas with two different isotopic characteristics.

The initial ratio  $(^{87}\text{Sr}/^{86}\text{Sr})_i$ , corrected for a 250 Ma is 0.710–0.712 and give evidence for crust dominated source of the magma.

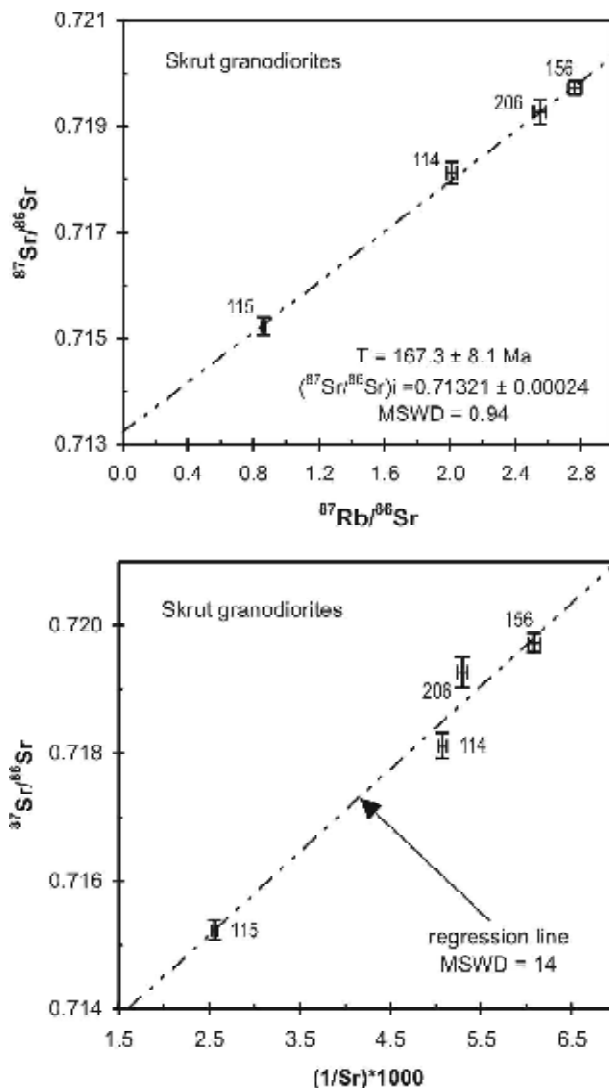
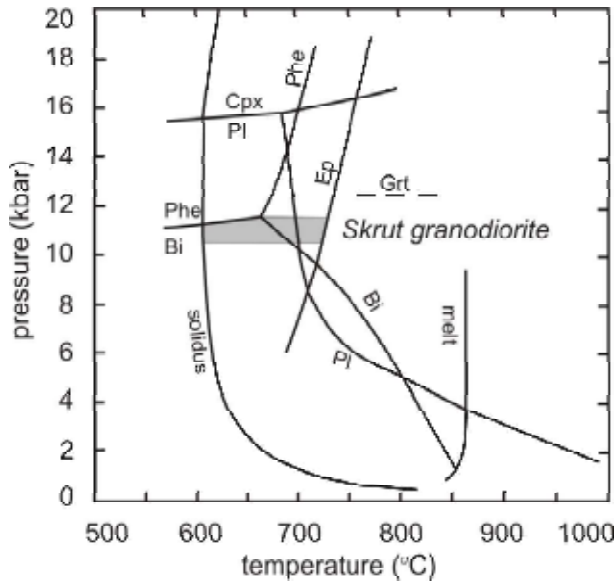


Fig. 10. Rb-Sr isotope data for Skrut granitoides. a) Isochrone diagram  $^{87}\text{Rb}/^{86}\text{Sr}$  vs.  $^{87}\text{Sr}/^{86}\text{Sr}$ ; b) Control for mixing of the magma components in  $(1/\text{Sr} \cdot 1000)$  vs.  $^{87}\text{Sr}/^{86}\text{Sr}$  coordinates

## P-T conditions of magma generation

The geochemical, isotopic, and petrographic features of the rocks were used to define the P-T conditions of magma generation of the Skrut granitoids. The mineral paragenesis of epidote minerals and biotite and the absence of amphibole suggest for water saturated magma (Naney, 1983). To evaluate the P-T conditions of crystallization of the granitoids we used the existing experimental data for water-saturated melts with granodioritic composition, which correspond to the established sequence of mineral crystallization epidote  $\rightarrow$  plagioclase  $\rightarrow$  biotite  $\rightarrow$  quartz  $\rightarrow$  alkali feldspar (Schmidt, Thompson, 1996). Except the temperature determinative for them are the lithostatic pressure, the partial pressure of water ( $P_{\text{H}_2\text{O}}$ ) and the fugacity of oxygen ( $f_{\text{O}_2}$ ) and it was accepted that  $P_{\text{H}_2\text{O}}$  is equal or higher than the lithostatic pressure. The published PT diagram (Schmidt, Thompson, 1996) (Fig. 11) shows that the crystallization sequence epidote  $\rightarrow$  plagioclase  $\rightarrow$  biotite has proceeded in a very narrow intervals of  $P_{\text{H}_2\text{O}}$  (11–11.5 kbar) and  $T^\circ\text{C}$  (730–660) and the solidus is reached at  $610^\circ\text{C}$ . The calculated temperatures for saturation of the magma with zirconium and the beginning of the zircon crystalli-



**Fig. 11.** Field of crystallization of Skrut granodiorites (epidote → plagioclase → biotite) on the pressure-temperature diagram for granodiorite melting at water-saturated conditions with  $f_{O_2}$  buffered by NNO (after Schmidt, Thompson, 1996)

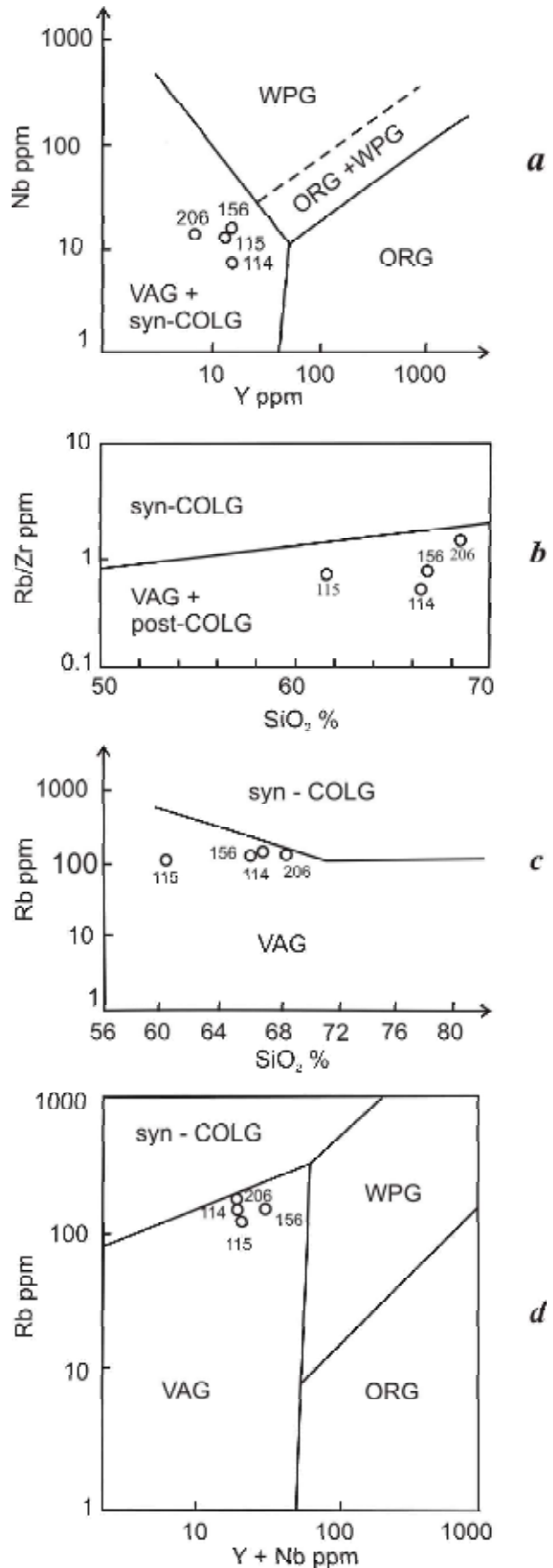
zation (Watson and Harrison, 1983) show even greater values up to about 800°C (Peytcheva et al., 2005), which correspond probably to a crust – magma generation. It is apparent that the crystallization of zircon continues also at lower temperatures as seen from the low-valued I.T indices (Fig. 5), which correspond to temperatures of 750–600°C. For the crystallization sequence plagioclase → biotite → quartz → alkali feldspar Pivinskii (1973, Fig. 2) determines maximal pressure of 7.5 kbar and temperature interval of 735–670°C with solidus at 650°C. On the basis of experiments in the system quartz → albite → orthoclase → anorthite → water at  $P_{H_2O}=7$  kbar Winkler et al. (1973, Fig. 6) have determined a temperature interval of 735–635°C.

The above data outline a crystallization trend for Skrut granitoids that starts at high pressures 11–11.5 kbar (the field of stability of epidote in magmatic conditions) and temperatures 800–750°C (temperature of saturation of zircon) and continues up to pressures of 7–7.5 kbar and temperatures of 600–650°C.

Discriminant diagrams and different rock characteristics are used for interpretation of the geodynamic



**Fig. 12.** Position of the Skrut granodiorites on the discriminant diagrams for geodynamic position of granitoid formation: a, c, d – after Pearce et al., 1984, b – after Harris et al., 1986; Abbreviations: syn-COLG – sin-collision, post-COLG – post-collision, VAG – volcanic arc, ORG – ocean ridge, WPG – within plate



environment of granitoid formation. The chemistry of the major elements and especially their slight peraluminous character, the presence of garnet and the initial strontium ratios give evidence that Skrut granitoids have been formed through crystallization of crustal dominated magma. From another side, the positive  $\varepsilon$ -Hf values of zircons speak in favour of participation of mantle component as well. In respect to the position of the samples on the discriminant diagram (Fig. 12a; Pearce et al., 1984) the Skrut granitoids belong to fields of volcanic-arc (VAG) and syn-collision (synCol) granites, but on diagrams, which allow discrimination of VAG and synCol they are clearly differentiated in the field of VAG to post-collision (postCol) granites (Fig. 12b, c, d). Consequently volcanic-arc/continental margin or post-collisional geotectonic environment could better explain the geochemical and isotope characteristics of Skrut granitoids, revealing mantle-crust signature, but with considerable participation of continental crust materials.

## Discussion

The formation of granitoid magmatism with Early Triassic age in SMM gives opportunity to look in a new way on the Late Variscan development of the region (the newest Time Scale of the International Commission on Stratigraphy determines the Permian-Triassic boundary at  $251 \pm 0.4$  Ma, Gradstein et al., 2004).

Up to now, several granitoid bodies intruded in high-metamorphic rocks from different levels of the Pre-Alpine basement are determined by U-Pb zircon dating to be of a similar ages, namely  $248.85 \pm 0.70$  Ma for Skrut granitoids,  $240 + 13/-9$  Ma for Igralishte pluton (Zidarov et al., 2004), and  $247 \pm 2$  Ma for Kerkini granite complex in Northern Greece (Christofidies et al., 2006). For Ograzhden batolith and the similar granitoid bodies in Belasitsa Mt. on the territory of Republic of Macedonia, an age of 234 Ma has been reported (Bogdanov, 1983, p.70), but Boev et al. (2002) have related them to the Early Paleozoic granite-granodiorite formation.

Skrut granitoids could be correlated also with the Arnea granites, exposed in Northern Greece close to the western boundary of SMM. They are dated by Kostopoulus et al. (2001) to be of an age of  $215.0 \pm 1.8$  Ma (Pb-Pb zircon method) and by Himmerkus et al. (2003) as being of an age from 210 to 230 Ma (single zircon evaporation method), i.e. as Late Triassic. The Rb-Sr whole rock analyses yield Jurassic age of  $155 \pm 11$  Ma (DeWet et al., 1988).

Permian-Triassic ages have been reported for I-type metagranites with imposed Late Alpine metamorphism from Central Rhodopes (Cherneva et al., 1991) as well as for metadiorites from the Ardino lithotectonic unit in Western Rhodopes —  $253 \pm 13$  Ma (von Quadt, Peytcheva, 2005). Similar age of  $245.6 \pm 3.9$  Ma and  $255.8 \pm 2.1$  Ma have been determined also for the amphibolitized and eclogitized gabbro in the western part of the Greek Rhodopes (Liati et al.,

2005) and for metabasites from their eastern part (Liati, Fanning, 2005).

It is known that the formation of the Cimmerian orogen on the Balkan peninsula has started almost at the same time with the on-set of the Tethyan basin, i.e. from the end of Permian or the beginning of Middle Triassic (Gochev, 1991) when the passive continental boundary of the Paleomoesian carbonate platform developed. Triassic sediments therein have been affected by the Early Cimmerian folding and thrusting (Dabovski et al., 2002). According to Gochev (1991) the Early Cimmerian orogen has started to form during Early Triassic but developed mainly during Middle Triassic. This formation is one “embryonic tectogen” that includes inner platforms and a system of peripheral island arcs and troughs; the earliest movements have formed the primary fault-block mosaic of micro-plates as well as their deformation. Closely related is the formation of some separate embryonic orogens with block-mosaic fold structure, which mark the edge of the European continental platform.

Probably, parts of the Cimmerian orogen are reworked during later Alpine epochs and has been included in the Rhodope and Serbo-Macedonian Massifs, as inferred from the cited geochronological data.

The early phases of the opening of the Mesozoic oceanic basin in Vardar-Axios zone near the western boundary of SMM have been accompanied by Triassic sedimentation and volcanism. The sedimentation has proceeded in a continental environment, which indicates extension, block faulting and formation of a basin at the end of Permian and the beginning of Triassic (rifting?). The basic volcanism has been activated during Late Triassic, when the rifting has been followed by oceanic spreading ongoing up to Middle-Late Jurassic and accompanied by east directed subduction (Dimitriadis, Asvesta, 1993).

Liati (2005) proposed two alternative scenarios for the generation of the gabbroid protoliths of the amphibolitized eclogites: (i) as part of a Late Permian/ Early Triassic ocean, or (ii) as a consequence of underplating, which associates with Permian-Triassic rifting. Himmerkus et al. (2003) interpreted their geochemical data for Arnea granite also with rifting and formation of within-plate granites (WPG).

Our data do not exclude the existence of a possible rifting at the end of Permian and the beginning of Triassic times along the western rim of SMM because the calc-alkaline trend of Skrut and Igralishte granitoids suggests the extension of the lithosphere. From another side, the discriminant diagrams (Fig. 12) determine the Skrut granitoids as volcanic-arc/continental margin or post-collisional (Pearce et al., 1984). These geochemical data support the idea of Gochev (1991) for “embryonal tectogen” that includes inner platforms and a system of peripheral island-arcs and troughs. Future studies could probably clarify the geodynamic reconstructions of the region during the earliest stage of the Cimmerian orogenesis.

In respect to the Rb-Sr whole-rock data of Skrut granitoids which yielded a Jurassic age, different explanation could be proposed. One of them supposes mixing of magmas with different isotopic characteristics. Another one assumes overprinting tectonic or metamorphic events, related for example to the subduction in the Vardar zone, or being a result of uplifting hot mantle magmas. It is possible also that we have calculated an errorchrone, which is partly rejuvenated during the Late Alpine processes. In this case the obtained age has no geological meaning (the calculated age is between the time of crystallization of granitoids and the time of the imposed alteration). The available data set and geochemical data for mixed mantle-crustal source argue for a most probable explanation of the Rb-Sr errorchrone with a mixing line but the final elucidation of this problem needs additional studies on the overprinting processes (for example — mineral Rb-Sr isochrones, Ar-Ar mineral studies, etc.).

The Jurassic ages are not unexpected for the Serbo-Macedonian Massif and the adjacent Vardar zone. Small granitoid plutons with calc-alkaline affinities of Late Jurassic and Early Cretaceous age (173–148 Ma) have been recognized along the southwest boundary of the Serbo-Macedonian Massif or in the adjacent Vardar zone in Republic of Macedonia. There the Stip granite is dated at  $161 \pm 3$  Ma and the granite near Furka at  $173 \pm 7$  Ma (Rb/Sr data of Spray et al., 1984). Similar ages are published for some granitoid plutons in northern Greece. The granite near Fanos, which is intruded in the Guevgueli ophiolite complex of the Vardar zone shows ages of  $148 \pm 3$  Ma (K/Ar biotite data; Spray et al, 1984) and  $150 \pm 2$  Ma (K/Ar and Rb/Sr biotite data; Borsi et al., 1966). Both ages have been interpreted by Anders et al. (2005) as connected with the cooling of the pluton and with later overprinting processes, whereas the intrusion age is obtained by zircon dating at  $158 \pm 1$  Ma. As mentioned above Late Jurassic age was calculated previously for the deformed Arnea granite by De

Welt et al. (1989), using Rb-Sr whole rock data, but this age was later corrected to Late Triassic. This fact raises the question about the real Jurassic age of other weakly deformed granitoids in SMM as their previous Rb-Sr or K-Ar age determinations may result from tectonic or thermal overprint, connected with the subduction of the Vardar ocean or other Alpine processes.

## Conclusion

1. The Skrut granitoids belong to the high potassium calc-alkaline magmatic series.
2. They are formed from water-saturated magma with the participation of a significant quantity of crust material and of subordinate quantity of mantle component.
3. Their crystallization has probably started at pressure 11.0–11.5 kbar, corresponding to a depth of more than 30 km and proceeded in a temperature interval of 800–600°C.
4. The age of their crystallization is determined by conventional U-Pb method on single zircons at  $248.85 \pm 0.70$  Ma.
5. Rb-Sr whole rock isotope analyses determine an “isochrone” that corresponds to  $167.3 \pm 8.1$  Ma, which can be interpreted as a mixing line or as influenced by later tectonic and thermal events.
6. The tectonic discriminations favor island-arc/continental margin or postcollisional geodynamic environment of magma generation.
7. Regional-geological data give evidence for extensional or rifting processes during Early Triassic time, which lead to formation of inner platforms and a system of peripheral island arcs and troughs.
8. Skrut granitoids are only weakly metamorphosed. They intrude the high-grade metamorphic rocks in Belasitsa Mountain defining the metamorphism of the latter as pre-Triassic in age.

## References

- Anders, B., Reischmann, T., Poller, U., Kostopoulos, D. 2005. Age and origin of granitic rocks of the Eastern Vardar Zone, Greece: new constraints on the evolution of the Internal Hellenides. — *J. Geol. Soc. London*, 162; 857–870.
- Abdel-Rahman, A. M. 1994. Nature of biotites from alkaline, calc-alkaline, and peraluminous magmas. — *J. Petrol.*, 35, 2; 525–541.
- Belousova, E., Griffin, W., O'Reilly, S., Fisher, N. 2002. Igneous zircon: trace element composition as an indicator of source rock type. — *Contrib. Mineral. Petrol.*, 143; 602–622.
- Boev, B., Lepitkova, S., Petrov, G. 2002. Granitoid formations in the Republic of Macedonia. — *Geol. Carpathica*, 53, CD version.
- Bogatnikov O. A., Michailov, N. P., Gonshakova, V. I. (eds). 1981. Classification and Nomenclature of Magmatic rocks. Moscow, Nedra, 160 pp. (in Russian)
- Bogdanov B. (Editor) 1983. *Magmatism and metallogeny of the Carpathian-Balkan area*. Bulgarian Acad. Sci. Publ. House, 300 (in Russian with English abstract).
- Bonchev G. 1920. Petrographic and mineral studies in Macedonia. — *Proceeding of Bulgarian Acad. of Sciences*, XIII, 5; 1–295. (in Bulgarian with abstract in German).
- Borsi, S., Ferrara, G., Mercier, J., Tongiori, E. 1966. Age stratigraphique et radiometrique Jurassique supérieur d'un granite des zones internes des Hellénides (granite de Fanos, Macédoine, Grece). — *Rev. Geog. Phys. Geol. Dyn.*, 8; 279–287.
- Cherneva, Z., Kotov, A. B., Vinogradov, D. P., Salnikova, E. B. 1991. Metamorphosed I-granites from the Central Rhodopes, Bulgaria. — *Compt. rend. Acad. bulg. Sci.*, 44, 10; 85–88.
- Christofidies, G., Koroneos, A., Liati, A., Kral, J. 2006. Geochronology of the Kerkini granitic complex (Serbomacedonian Massif, N. Greece) and geodynamic implications. — *Proceedings XVIIIth congress of the Capathian-Balkan Geological Association*, September 3–6, 2006, Belgrade, Serbia.
- Dabovski, C., Boyanov, I., Khrichev, Kh., Nikolov, T., Sapounov, I., Yanev, Y., Zagorchev, I. 2002. Structure and Alpine evolution of Bulgaria. — *Geol. Balc.*, 32, 2–4; 9–15.

- De Wet, A. P., Miller, J. A., Bickle, M. J., Charman, H. J. 1989. Geology and geochronology of the Arnea, Sithonia and Ouranopolis intrusions, Chalkidiki Peninsula, northern Greece. *Tectonophysics*, 161; 65–79.
- Dimitriadis, S., Asvesta, A. 1993. Sedimentation and magmatism related to the Triassic rifting and later events in the Vardar-Axios zone. — *Bull. Geol. Soc. Greece*, 28, 2; 149–168.
- Dimovski, S., Sevdanov, S. 2002. Elements of the geological structure of Belassitsa-Ograzhden block in respect to complex geophysical data. — *Ann. Univ. Mining and Geology*, 45, I, Geology, 109–116 (in Bulgarian with English abstract)
- Gochev, P. 1991. The Alpine orogen in the Balkans — a polyphase collisional structure. — *Geotect., Tectonophys. and Geodinamics*, 22; 3–44.
- Gradstein, J. G., Ogg, A. G., Smith, A. 2004. *The geological time scale*. Cambridge University Press.
- Harris, N., Pearce, J., Tindle, A. 1986. Geochemical characteristics of collision-zone magmatism. — In: *Coward, M. A., Ries, A. C.* (Eds), *Collision Tectonics*, *Geol. Soc. London Spec. Publ.*, 19; 67–81.
- Himmerkus, F., Reischmann, T., Kostopoulos, D. 2003. The Serbo-Macedonian Massif, the oldest crustal segment of the internal Hellenides, identified by zircon ages. — *Geophys. Research Abstr.*, 5, 05671.
- Hoskin, P., Ireland, T. 2000. Rare earth chemistry of zircon and its use as a provenance indicator. — *Geology*, 28, 7; 627–630.
- Kostopoulos, D. K., Reischmann, T., Sklavounos, S. A. 2001. Palaeozoic and Early Mesozoic magmatism and metamorphism in the Serbo-Macedonian massif, Central Macedonia, Northern Greece. — *European Union of Geosciences, Abstracts*, LS03: Tham 01:F2, p. 318.
- Kozhukharov, D., Kozhoukharova, E., Vergilov, V., Zagorchev, I. 1974. On the lithostratigraphic grouping of the Precambrian in Bulgaria. — In: Zoubek, V. (Ed.), *PICG, Precambrian des zones mobiles de l'Europe*, Conf. Liblice 1972; 233–240.
- Le Maitre, W. (ed.). 1989. *A Classification of Igneous Rocks and Glossary of Terms*. Recommendations of the IUGS Subcommission on the Systematics of Igneous Rocks. Oxford, Blackwell Sci. Publ., 193 p.
- Liati, A. 2005. Identification of related Alpine (ultra) high-pressure metamorphic events by U-Pb SHRIMP geochronology and REE geochemistry of zircon: the Rhodope zone of Northern Greece. — *Contrib. Mineral. Petrol.* 150; 608–630.
- Liati, A., Fanning, M. 2005. Eclogites and country rock orthogneisses representing Upper Permian gabbros in Hercynian granulites, Rhodope, Greece: Geochronological constraints. — *Abstr. Mitt. Österr. Miner. Ges.*, 88.
- Ludwig, K. R. 1998. Isoplot/Ex, Version 1.00 — *A Geochronological Toolkit for Microsoft Excel*. Berkeley Geochronological Center Special Publication, 1; 43 p.
- Maniar, P. D., Piccoli, P. M. 1989. Tectonic discrimination of granulites. — *G.S.A.B.*, 101; 635–643.
- Metasomatism and metasomatic rocks*. 1998. Moscow, Nauchnii mir, 489 pp. (in Russian).
- Pearce, J., Harris, N., Tindle, A. 1984. Trace element discrimination diagrams for the tectonic interpretation of granitic rocks. — *J. Petrol.*, 25; 956–983.
- Peccerillo, A., Taylor, S. R. 1976. Geochemistry of Eocene calc-alkaline volcanic rocks from the Kastamonu area, Northern Turkey. — *Contr. Mineral. Petrol.*, 110; 304–310.
- Peytcheva, I., von Quadt, A., Titorenkova, R., Zidarov, N., Tarassova, E. 2005. Skrut granulites from Belassitsa Mountains, SW Bulgaria: Constraints from isotope-geochronological and geochemical zircon data. — *Proc. Jubilee Intern. Conf. "80 years BGS"*, Sofia, 109–112.
- Pirjano, F. 1992. *Hydrothermal Mineral Deposits. Principles and Fundamental Concepts for Exploration Geologist*. Springer-Verlag, Berlin; 709 p.
- Piwinskii, A. J. 1973. Experimental studies of igneous rock series, central Sierra Nevada batholith, California. Part II. — *N. Jb. Miner. Mh.*, 5; 193–215.
- Pupin, J-P. 1980. Zircon and granite petrology. — *Contrib. Mineral. Petrol.*, 73; 207–220.
- Schmidt, M. W., Thompson, A. B. 1996. Epidote in calc-alkaline magmas: An experimental study of stability, phase relationships, and the role of epidote in magmatic evolution. — *Am. Mineral.*, 81; 462–474.
- Spray, J. G., Bebie, J., Rex, D. C., Roddick, J. C. 1984. Age constraints on the igneous and metamorphic evolution of the Eastern Mediterranean. — *Geol. Soc. London Spec. Publ.*, 17, Blackwell Scientific Publications, Oxford; 619–627.
- Tarassova, E., Tarassov, M. 2004. Accessory allanite and its petrogenetic significance for granulites from Belassitsa Mountain, Serbo-Macedonian Massif. — *5<sup>th</sup> ISEMG*, Thessaloniki, Greece, 3; 1248–1251.
- Tarassova, E., Zidarov, N., Khaltakova, N. 2001. I-type granulites from the Belassitsa Mountain, SW Bulgaria. — *Geochem. Miner. Petrol.*, 38; 79–89.
- Von Quadt, A., Peytcheva, I. 2005. The southern extension of the Srednogorie type Upper Cretaceous magmatism in Rila-Western Rhodopes: Constraints from isotope-geochronological and geochemical data. — *Proc. Jubilee Intern. Conf. "80 years BGS"*, Sofia; 113–116.
- Winkler, H. G., Boese, M., Markopoulos, T. 1975. Low temperature granitic melts. — *N. Jb. Miner. Mh.*, 5; 245–268.
- Watson, E. B., Harrison, T. M. 1983. Zircon saturation revisited: temperature and composition effects in variety of crustal magma types. — *Earth Planet. Sci. Lett.*, 64, 2; 295–304.
- Zagorchev, I. 1976. Tectonic, metamorphic and magmatic markers in the polycyclic ultrametamorphic Ograzdenian complex. — *Geologica Balc.*, 6, 2; 17–34.
- Zagorchev, I., Dinkova, J. 1991. *Geological map of Bulgaria, M 1: 100 000, Sheet Petric*.
- Zagorchev, I., Dinkova, J. 1990. *Explanatory note to the geological map of Bulgaria 1: 100 000. Sheet Petric (together with Strumica and Sidirokastron)*. Sofia, 38 p. (in Bulgarian).
- Zagorchev, I. 1992. Neotectonic development of the Struma (Kraïštide) Lineament, Southwest Bulgaria and Northern Greece. — *Geol. Mag.*, 129, 2; 197–222.
- Zagorchev, I. 2001. Introduction to the geology of SW Bulgaria. — *Geologica Balc.*, 31, 1–2; 3–52.
- Zharikov, V. A., Omelyanenko, B. I. 1978. Classification of metasomatites. — In: *Metasomatism and ore formation*. — M., Nauka, 9–28 (in Russian).
- Zidarov, N., Kostov, I., Stoeva, V., Marinov, L., Karaivanova, R., Dimitrov, D., Ignatovski P. 1966. Report on the geology of Belassitsa Mountains and Southern parts of Ograzhden mountains (geological mapping and ore deposits exploration, M 1:25 000), National Geofund, 262 p. (in Bulgarian).
- Zidarov, N., Andreichev, V., Tarassova, E. 2002. Rb-Sr date for Jurassic granitic bodies in Belassitsa Mountain, SW Bulgaria. — In: *Modern problems of the Bulgarian geology. Annual scientific conference of BGS*; 23.
- Zidarov, N., Peytcheva, I., von Quadt, A., Tarassova, E., Andreichev, V. 2004. Timing and magma sources of Igralishte pluton (SW Bulgaria): preliminary isotope-geochronological and geochemical data. — *J. Bulg. Geol. Soc. Ann. Scient. Conference "Geology 2004"*, Dec. 16–17, Sofia; 116–118.